



Combining offshore wind and solar photovoltaic energy to stabilize energy supply under climate change scenarios: A case study on the western Iberian Peninsula

X. Costoya^{a,b,*}, M. deCastro^b, D. Carvalho^c, B. Arguilé-Pérez^b, M. Gómez-Gesteira^b

^a CRETUS, Group of Nonlinear Physics, Faculty of Physics, University of Santiago de Compostela, 15782, Santiago de Compostela, Spain

^b Centro de Investigación Mariña, Universidade de Vigo, Environmental Physics Laboratory (EPhysLab), Campus da Auga, 32004, Ourense, Spain

^c CESAM, Physics Department, University of Aveiro, 3810-193, Aveiro, Portugal

ARTICLE INFO

Keywords:

Offshore wind energy
Solar energy
CORDEX
Climate change
West Iberian Peninsula
Climate projections

ABSTRACT

The expansion of marine renewable power is a major alternative for the reduction of greenhouse gases emissions. In Europe, however, the high penetration of offshore wind brings intermittency and power variability into the existing power grid. Offshore solar photovoltaic power is another technological alternative under consideration in the plans for decarbonization. However, future variations in wind, air temperature or solar radiation due to climate change will have a great impact on both renewable energy resources. In this context, this study focusses on the offshore energy assessment off the coast of Western Iberia, a European region encompassing Portugal and the Northwestern part of Spain. Making use of a vast source of data from 35 simulations of a research project called CORDEX, this study investigates the complementarity of offshore wind and solar energy sources with the aim of improving the energy supply stability of this region up to 2040. Although the offshore wind energy resource has proven to be higher than solar photovoltaic resource at annual scale, both renewable resources showed significant spatiotemporal energy variability throughout the western Iberian Peninsula. When both renewable resources are combined, the stability of the energy resource increased considerably throughout the year. The proposed wind and solar combination scheme is assessed by a performance classification method called Delphi, considering stability, resource, risk, and economic factors. The total index classification increases when resource stability is improved by considering hybrid offshore wind-photovoltaic solar energy production, especially along the nearshore waters.

1. Introduction

European Union decarbonization plans set ambitious targets to reduce by at least 40% greenhouse gases emission by 2030, when compared to 1990 levels [1], and to reach long-term climate neutrality by 2050 [2]. To achieve these goals, upscaling and fully optimizing the renewable power generation is crucial. Europe currently has 573.3 GW of renewable power generation capacity, the second largest in the world, with solar, hydroelectric, and onshore wind accounting for approximately 93% of the total [3,4]. The EU strategic roadmap estimates that 10% (100 GW) of European Union electricity consumption by 2050 can be potentially supported by offshore renewables [5]. The diversification of energy sources by marine renewables thus plays a promising role in this roadmap.

Offshore wind energy is the most mature marine renewable source, as it is the only one that has reached an established commercialization stage in Europe [4]. In fact, Europe is the birthplace and the leader of the offshore wind industry, with 75% of the total global offshore wind installation in 2019 [6] and 25 GW of installed capacity in 2020 [7]. However, the distribution of offshore wind farms is not homogenous along the European Atlantic Arc. The United Kingdom, Germany, and Denmark account for more than 70% of offshore wind farms installed in Europe [7]. Therefore, this offshore energy resource is clearly more developed in northern Europe than in the south, despite the fact that some areas such as the western Iberian Peninsula show a high offshore wind energy resource potential [8,9], comparable to the resource in the North Sea. This underdevelopment in the Iberian Peninsula can be explained, among other facts, by its narrow continental shelf and deep waters, which preclude the installation of offshore wind turbines over

* Corresponding author. CRETUS, Group of Nonlinear Physics, Faculty of Physics, University of Santiago de Compostela, 15782, Santiago de Compostela, Spain.
E-mail addresses: jorge.costoya.noguerol@usc.es, xurxocostoya@uvigo.es (X. Costoya).

<https://doi.org/10.1016/j.rser.2021.112037>

Received 31 May 2021; Received in revised form 18 October 2021; Accepted 21 December 2021

Available online 5 January 2022

1364-0321/© 2021 The Authors. Published by Elsevier Ltd. This is an open access article under the CC BY license (<http://creativecommons.org/licenses/by/4.0/>).

Nomenclature			
CORDEX	coordinated regional climate downscaling experiment	RCP	representative concentration pathways
C_v	coefficient of variation index	OP	overlap percentage
DC	distance to coast	PDF	Probability density function
ECMWF	european centre for medium-range weather forecasts	PV	Photovoltaic
EWS	extreme wind speeds	PVres	Photovoltaic solar power resource
EWSO	frequency of occurrence of effective wind speed	RCMs	regional climate models
GCMs	global climate models	RLO	rich level occurrence
hPa	hectopascal	W	Watts
M_v	monthly variability index	W_{ann}	annual average wind speed
NREL	national renewable energy laboratory	WD	water depth
		WPD	wind power density
		WRF	weather research and forecasting model

monopiles or jackets fixed in the seabed. However, technical progresses in offshore wind structures has already allowed the installation of the first floating offshore wind farm in the Iberian Peninsula, more precisely in Portugal [7].

In the upcoming decades, the technological evolution of floating offshore wind turbines is expected to promote and foster new offshore wind farms in the western coastal area of Iberia. Numerous studies have already quantified the offshore wind energy resource in this area using past wind data [9–12]. In addition, the influence of climate change on the future development of offshore wind farms in this area was also previously investigated using data from the Coordinated Regional Downscaling Experiment (CORDEX) project [8,13,14]. This is an important point since small changes in wind speed can have a significant impact on the wind energy that a wind turbine can generate because it depends on the cube of the wind speed. The aforementioned studies reported a global decrease in the offshore wind potential for the next decades in the western Iberia, with the exception of its northwestern areas where null changes or even an increase were projected. In addition to the assessment of the offshore wind energy resource, the legal framework [15,16] and the economic feasibility of the installation of floating wind farms on the western coast of the Iberian Peninsula were also analyzed [17], also considering the impact of future climate change [18].

An associated drawback of offshore wind energy farms is their intermittence and variability in energy production throughout the year (known as inter-annual variability or seasonality). This is a key factor since offshore wind energy storage and integration in the electrical grid continues to be a challenge [19], and it becomes particularly critical considering that, to reach the decarbonization plans previously mentioned, the relevance of renewable energy resources over the European countries energy mix will grow considerably. Hybrid offshore energy systems based on the combination of two or more marine renewable sources can reduce this inter-annual variability, installation and maintenance costs [20]. Offshore hybrid power systems have already been proposed and investigated in different combinations [21, 22]. However, to the best knowledge of the authors of this article, none of these prototypes have been commercially deployed yet. The main reason is that marine technologies such as wave and tidal converters are still relatively far away from technological readiness [4]. Recently, different combinations of wind and solar photovoltaic (PV) power in offshore platforms have been proposed in the technical literature [e.g. 22, 23]. The main strength of the offshore wind and PV solar mix is that both renewable sources are at a high level of technological maturity.

China has already started promoting offshore photovoltaic exploration in its coastal areas. Wu et al. [24] analyzed the potential risks associated with the installation of PV panels along the Chinese coast, pointing out that PV panels installed at the sea waterline keep in low temperature, and thus operate with higher efficiency. This increase in efficiency was also corroborated by Golroodbari & vanSark [25] who concluded that a PV system at sea performs ~13% better on average

than a land-based system. Oliveira-Pinto et al. [26] investigated the possibility of combining wave and PV solar energy at sea to supply energy to offshore oil and gas platforms. These authors also highlighted the increasing focus on the use of floating PV solar energy in ocean locations, as more technological advances are being reached in this field. For example, Trapani & Millar [27] proposed the use of a flexible, thin, and innovative floating PV. Detailed information on recent technical advances regarding floating PV panels can be found in Gorjian et al. [28]. It is important to mention that the first prototype of an offshore floating solar farm has been tested in the rough Dutch North Sea [29]. Furthermore, the Netherlands considered floating offshore PV as an option in its national roadmap on PV potential, defining an offshore potential of 45 GW [30]. Following this trend of considering offshore PV solar energy resource as a viable option, Golroodbari et al. [22] have recently analyzed the integration of a floating PV farm within an offshore wind farm in the Dutch North Sea. They concluded that it presents technical and economic benefits, such as a higher use rate of the cable that transports electricity to the coast. López et al. [31] also studied the synergies of combining floating offshore wind and solar PV in a region to the north of Spain (Asturias). They took the basic approach of filling the free-surface between the wind turbines with floating PV panels. These authors concluded that this hybrid system increases both the power output per unit area and its quality. In addition, López et al. [31] evaluated the offshore PV solar energy resource by mapping the average irradiance (Wm^{-2}). This methodology was followed in other areas of the world, such as India [32], with the aim of knowing the offshore PV solar energy resource, which is the first step for its exploitation.

The purpose of this study is to analyze the advantages of an offshore hybrid farm that combines wind turbines and PV solar panels on the western coast of the Iberian Peninsula, since it is expected a rapid growth in the number of offshore wind farms projects in this area in the upcoming decades. This study was carried out using regional climate models from the CORDEX project over the period 2000–2040. The selected period covers both the recent past and the effects that climate change can have on renewable energy resource in the upcoming decades [8,14,18,33]. The proposed hybrid farm is assessed by a performance classification method called Delphi, considering stability, resource, risk, and economic factors. The water depth, which is one of the major cost factors and site selection criteria, is also a relevant input for our study case about offshore renewable energy resources off the western coast of the Iberian Peninsula (Fig. 1, in meters).

2. Data and methods

2.1. Data

Three different atmospheric variables were used to perform the present analysis: wind speed measured at 10 m above sea level, the temperature measured at 2 m above sea level, and surface downwelling

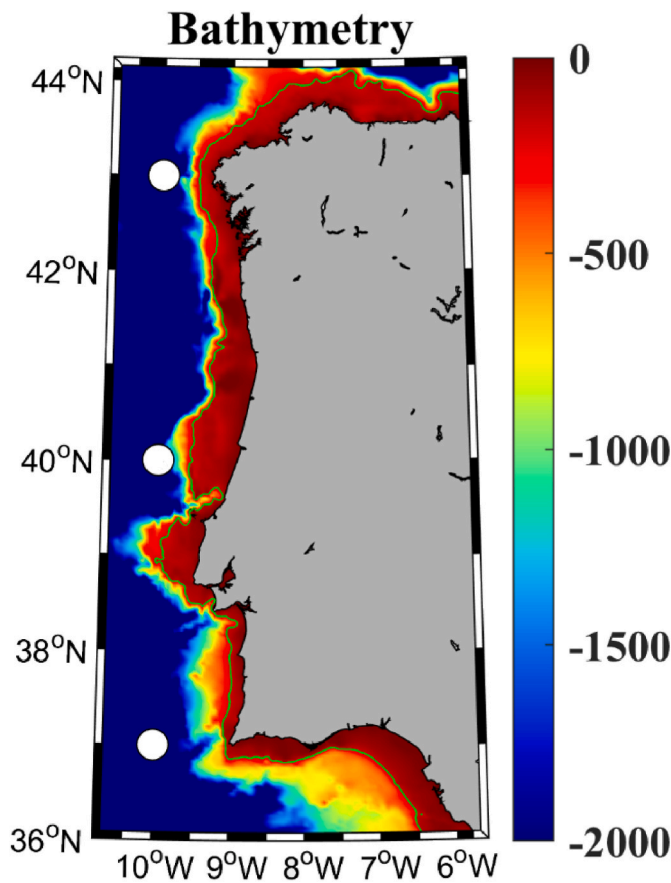


Fig. 1. Area under scope and bathymetry (in meters). The green line represents 200 m isobaths. White dots indicate the locations selected to carry out the monthly analysis of wind and solar power resources.

shortwave radiation. These data were obtained from regional climate simulations carried out within the framework of the EURO-CORDEX project [34], which is the European branch of the CORDEX initiative. Simulations that met the following requisites were selected: daily resolution, 0.11° of spatial resolution, and simulations with the three variables available both for the historical and future period under the most pessimistic greenhouse gases emissions scenario (RCP8.5). This scenario assumes that the greenhouse gas emission will lead, in 2100, to a radiative forcing of 8.5 Wm⁻². A positive radiative forcing means that Earth receives more energy from sunlight that it radiates to space. Detailed information regarding future climate scenarios can be found in Henne-muth et al. [35]. A total of 35 simulations were selected after filtering all the available EURO-CORDEX data that met these requisites. Detailed information of each simulation can be found in Table 1. The period 2000–2040 was selected to analyze the combined wind and PV solar energy resources during the recent past and the influence of climate change in the near future.

In order to know the reliability of CORDEX simulations, the EURO-CORDEX data was compared and validated with ERA5 [36], the latest state-of-the-art reanalysis from the European Centre for Medium-Range Weather Forecasts (ECMWF). ERA5 provides data in a regular global grid with a horizontal resolution of 0.25° from 1979 onwards. The validation for the three variables was done for the common period between ERA5 and the historical simulations from the CORDEX project (1979–2005). Since ERA5 has a lower resolution, it is necessary to interpolate CORDEX data to the same grid points of ERA5. This interpolation only was done for the validation procedure, and the original resolution (0.11°) was used for the remaining analyses included in this study. The use of ERA5 to validate simulations from regional climate

Table 1
Regional climate simulations from EURO-CORDEX [34] project used in this study.

Model Number	Global Climate	Regional Climate	Institution
	Model (GCM)	Model (RCM)	
1	CNRM-CERFACS-CNRM-CM5	CCLM4-8-17	CLMcom
2	CNRM-CERFACS-CNRM-CM5	ALADIN63	CNRM
3	CNRM-CERFACS-CNRM-CM5	HIRHAM5	DMI
4	CNRM-CERFACS-CNRM-CM5	REMO2015	GERICS
5	CNRM-CERFACS-CNRM-CM5	WRF381P	IPSL
6	CNRM-CERFACS-CNRM-CM5	RACMO22E	KNMI
7	CNRM-CERFACS-CNRM-CM5	RCA4	SMHI
8	ICHEC-EC-EARTH	HIRHAM5	DMI
9	ICHEC-EC-EARTH	RACMO22E	KNMI
10	ICHEC-EC-EARTH	RCA4	SMHI
11	IPSL-IPSL-CM5A-MR	REMO2015	GERICS
12	IPSL-IPSL-CM5A-MR	WRF381P	IPSL
13	IPSL-IPSL-CM5A-MR	RACMO22E	KNMI
14	IPSL-IPSL-CM5A-MR	RCA4	SMHI
15	MOHC-HadGEM2-ES	CCLM4-8-17	CLMcom
16	MOHC-HadGEM2-ES	COSMO-crCLIM-v1-1	CLMcom-ETH
17	MOHC-HadGEM2-ES	ALADIN63	CNRM
18	MOHC-HadGEM2-ES	RegCM4-6	ICTP
19	MOHC-HadGEM2-ES	WRF381P	IPSL
20	MOHC-HadGEM2-ES	RACMO22E	KNMI
21	MOHC-HadGEM2-ES	RCA4	SMHI
22	MPI-M-MPI-ESM-LR	CCLM4-8-17	CLMcom
23	MPI-M-MPI-ESM-LR	COSMO-crCLIM-v1-1	CLMcom-ETH
24	MPI-M-MPI-ESM-LR	ALADIN63	CNRM
25	MPI-M-MPI-ESM-LR	HIRHAM5	DMI
26	MPI-M-MPI-ESM-LR	RegCM4-6	ICTP
27	MPI-M-MPI-ESM-LR	RACMO22E	KNMI
28	MPI-M-MPI-ESM-LR	REMO2009	MPI-CSC
29	MPI-M-MPI-ESM-LR	RCA4	SMHI
30	NCC-NorESM1-M	COSMO-crCLIM-v1-1	CLMcom-ETH
31	NCC-NorESM1-M	HIRHAM5	DMI
32	NCC-NorESM1-M	REMO2015	GERICS
33	NCC-NorESM1-M	WRF381P	IPSL
34	NCC-NorESM1-M	RACMO22E	KNMI
35	NCC-NorESM1-M	RCA4	SMHI

models was previously done by different studies around the world [37, 38].

2.2. Methods

2.2.1. Validation of CORDEX data

The wind speed, the air temperature and the shortwave downward radiation from the EURO-CORDEX simulations were compared with the corresponding variables from ERA5. An overlap percentage (OP) between EURO-CORDEX and ERA5 data was used as metric to validate EURO-CORDEX data. OP, based on the study carried out by Perkins et al. [39], compares the entire data distributions, and was previously used in other studies to validate CORDEX simulations [14,40]. This methodology is based on the calculation of the OP between two series, one from the RCM simulation and another from the reference database (ERA5 for the present case). OP calculation involves computing the probability density functions (PDFs) in defined ranges (bins) for each variable. After that, the lowest value for each bin is selected and finally, all the selected values for all bins are summed. This procedure is summarized in Eq. (1):

$$OP = \sum_1^n \text{minimum}(Z_m, Z_0) * 100 \quad (1)$$

where n is the number of bins used to calculate the PDFs of each variable, and Z_0 and Z_m are the frequency of values of the RCM ERA5 and simulation, respectively, for each bin. Therefore, an OP value of 100 means a perfectly match between simulation and the reference data.

2.2.2. Wind and solar photovoltaic energy resource calculation

Wind energy resource was estimated in terms of wind power density (WPD). An important advantage of this metric is that it only considers the wind energetic resource available in the atmosphere. Thus, it allows the comparison between different areas to select the most wind energetic regions. For this reason, WPD is the most common metric to characterize the wind energy resource. WPD was calculated following Eq. (2):

$$WPD = \frac{1}{2} \rho_a W_H^3 \quad (2)$$

where W_H is the wind speed at the hub height and ρ_a is the air density (1.225 kg m^{-3} at 288.15 K and 1000 hPa). The WPD was calculated at 120 m, which is the typical hub height of offshore wind farms [41,42], by extrapolating the speed data at 10 m of CORDEX. To carry out the extrapolation from 10 m to 120 m above sea level, the logarithmic wind profile equation was chosen:

$$W_H = W_{ns} \frac{\ln\left(\frac{H}{z_0}\right)}{\ln\left(\frac{H_{ns}}{z_0}\right)} \quad (3)$$

where W_{ns} is the near-surface wind speed (10 m for the present case); H is the selected hub height (120 m); H_{ns} is the original height (10 m for EURO-CORDEX winds); and z_0 is the roughness length. It was calculated empirically using ERA5 dataset since this database provides wind speed values at 10 m and 100 m. 10 m wind speed from ERA5 were extrapolated to 100 m by using an ample range of z_0 values, and the z_0 value that showed the lowest difference with the original ERA5 100 values was selected. The selected roughness length was 0.00004. Detailed information about this methodology can be found in Costoya et al. [38].

Photovoltaic solar power resource (PV_{res}) can be estimated considering the amount of shortwave downward radiation and a correction related to the efficiency of PV cells, which diminishes as their temperature increases [43]. Shortwave downward radiation is the variable that accounts for the energy received directly by the Earth's surface from the Sun in the form of ultraviolet and visible light. Although the Sun emits longwave and shortwave radiation, only the second one has the enough energy to produce electricity when hit a solar cell. Thus, PV_{res} was calculated following Jerez et al. [44] through the following equations:

$$PV_{res} = P_R * RSDS \quad (4)$$

where $RSDS$ refers to the shortwave downward radiation (W m^{-2}) and P_R is a performance ratio that accounts for the effect that temperature has on PV cells efficiency. It can be calculated following:

$$P_R = 1 + \gamma(T_{cell} - T_{STC}) \quad (5)$$

where γ is a fixed value of $-0.005 \text{ } ^\circ\text{C}^{-1}$ according to Tonui & Tripanagnostopoulos [45] who investigated the response of monocrystalline silicon solar panels. T_{STC} is a reference temperature assumed as $25 \text{ } ^\circ\text{C}$, whilst T_{cell} refers to the cell temperature that depends on air temperature, downward shortwave radiation and wind speed. It can be calculated following Chenni et al. [46] as:

$$T_{cell} = c_1 + c_2 * TAS + c_3 * RSDS + c_4 * WS \quad (6)$$

where TAS is the air temperature, WS refers to the wind speed, and c_1 ,

c_2 , c_3 , and c_4 has the following values: $4.3 \text{ } ^\circ\text{C}$, 0.943 , $0.028 \text{ } ^\circ\text{C m}^2 \text{ W}^{-1}$ and $-1.528 \text{ } ^\circ\text{C s m}^{-1}$, respectively. Detailed information on the methodology to calculate photovoltaic power generation can be found in Jerez et al., [44].

WPD and PV_{res} were calculated at daily scale for each grid point using a common grid with the same spatial resolution ($0.11^\circ \times 0.11^\circ$). Then, a multi-model approach was considered averaging WPD and PV_{res} data from the 35 simulations. Previous studies [47,48] have demonstrated that a multi-model approach reduces the uncertainty of individual simulations.

2.2.3. Offshore wind energy classification

Offshore wind energy resource along the west Iberian Peninsula coast was classified considering four criteria: stability of the resource, its richness, economical factors, and risk factors. This methodology is based on a Delphi approach, which is a decision technique based on the opinion of different experts. This approach was firstly implemented by Zheng et al. [49], and then, applied by Costoya et al. [38], Costoya et al. [50], and Ribeiro et al. [33] to classify the offshore wind energy in different coastal areas around the world. In brief, the classification index of the offshore wind energy resource for each grid point is based on the calculation of eight normalized indices, which are after multiplied by a weight determined by the Delphi and then added.

This study focuses mainly on the analysis of the stability of the offshore energy resource and its variability throughout the year. Two indices take into account the stability of the resource in this classification: C_v (coefficient of variation) and M_v (monthly variability index). The first one (C_v), is calculated as follows:

$$C_v = \frac{\sigma}{\bar{X}} \quad (7)$$

where σ refers to the standard deviation and \bar{X} to the daily mean wind speed value. Standard deviation was calculated as

$$\sigma = \sqrt{\frac{\sum_{i=1}^N |A_i - \bar{A}|^2}{N - 1}} \quad (8)$$

where A_i is each value of the wind speed series; \bar{A} is the mean value of A and N is the total number of elements of the series.

M_v considers the monthly WPD values and was calculated according to Eq. (9):

$$M_v = \frac{P_{M1} - P_{M12}}{P_{year}} \quad (9)$$

where P_{M12} and P_{M1} are the average WPD calculated in the months with the lowest and the highest mean WPD, respectively; whilst P_{year} is the annual average WPD.

Three indices were considered to evaluate the richness of the offshore wind energy resource. The first one (W_{ann}) is based on the classification developed by the NREL [51]. The second one (effective wind speed occurrence, EWSO) quantifies the frequency of occurrence of wind speeds between the typical cut-in (4 ms^{-1}) and cut-out velocity (25 ms^{-1}). Finally, the rich level occurrence (RLO) index considers the frequency of occurrence of 10 m WPD higher than 200 W m^{-2} . This threshold value of rich occurrence was selected based on previous analysis [38,52,53].

Regarding economic factors, two crucial aspects were considered in this classification: the distance to coast (DC) and the water depth (WD). In general, higher water depths or distances to coast involve higher costs for wind turbines installation and energy transportation to land. DC and WD indices were calculated using the Global Self-consistent, Hierarchical, High-resolution Geography coastline databases [54] and the Earth topography 1 arc minute bathymetry (ETOP01) [55], respectively.

Finally, the risk of offshore wind turbines associated with extreme

wind speeds was taken into account using the EWS index. Its calculation is based on the Gumbel curve method considering a return period of 50 years [56,57].

Now, it is necessary to normalize the eight indices in order to compare and combine them, since each index has different units and magnitudes. To carry out the normalization procedure 10 categories were selected for five indices (Table 2) and 5 ranges were chosen for the economic factors (Table 3). In addition, W_{ann} index was normalized following the seven categories originally used to define this index following NREL, [51]. According to the normalization procedure, a value of 1 is considered optimal, whilst a value of 0 is the worst.

Finally, normalized values were multiplied by the weight given to each index (Table 4) to obtain a final classification index for each grid point (Table 5). These weights were established following a Delphi method based on the inputs of ten experts in the field of offshore wind energy [49].

The final classification included seven categories according to Zheng et al. [49] (Table 5).

3. Results

3.1. Capability of CORDEX simulations to reproduce wind and solar PV data

The reliability of the EURO-CORDEX simulations to represent the three atmospheric variables used to calculate offshore wind and solar power resources was evaluated by comparing the data from each RCM simulation (Table 1) with the corresponding one from ERA5 reanalysis.

The multi-model OP (Eq. (1)) was calculated for each atmospheric variable and for each grid point of the area under scope (Fig. 2). In general, values greater than 80% were obtained in the entire area for the three variables. Regarding wind comparison, only small spots with slightly lower values, close to 75%, were observed in coastal areas (Fig. 2c). These OP values are similar to those obtained in previous analysis that also used the metric OP to validate CORDEX simulations by means of ERA reanalysis [8,38] or using *in-situ* data from buoys at sea [14,40].

All RCMs simulations were considered in the multi-model ensemble because the WPD and PV_{res} OP averaged for all grid points and for each numerical simulation is not lower than those of the multi-model mean minus 2 standard deviations, for both metrics in any simulation (see Appendix, Table A.1Table A1).

3.2. Wind and solar power resource

Offshore wind and solar power resource in the western Iberia were calculated through Eq. (2) and Eq. (4), respectively. Annual mean WPD greater than 200 Wm^{-2} , which is often considered a threshold value of rich occurrence [40,53], was observed in most of the region, except for some coastal areas in the northernmost part (Fig. 3a). The highest

Table 2

Normalized criterion used for stability indices (C_v and M_v), richness indices (RLO and EWSO) and risk index (EWS).

Normalized value	C_v	M_v	RLO (%)	EWSO (%)	EWS (ms^{-1})
0/9	>1.9	>2.5	<10	<10	>27
1/9	1.7–1.9	2.25–2.5	10–20	10–20	25.5–27.0
2/9	1.5–1.7	2.0–2.25	20–30	20–30	24.0–25.5
3/9	1.3–1.5	1.75–2.0	30–40	30–40	22.5–24.0
4/9	1.1–1.3	1.5–1.75	40–50	40–50	21.0–22.5
5/9	0.9–1.1	1.25–1.5	50–60	50–60	19.5–21.0
6/9	0.7–0.9	1.0–1.25	60–70	60–70	18.0–19.5
7/9	0.5–0.7	0.75–1.0	70–80	70–80	16.5–18.0
8/9	0.3–0.5	0.5–0.75	80–90	80–90	15.0–16.5
9/9	<0.3	<0.5	>90	>90	<15.0

Table 3

Normalized criterion used for cost factors: WD (water depth) and DC (distance to coast).

Normalized value	WD	DC
	(m)	(°)
0	>500	>4
0.25	100–500	3–4
0.5	50–100	2–3
0.75	25–50	0.5–2
1	0–25	<0.5

Table 4

Weight coefficient for the wind energy classification.

	W_{ann}	EWSO	RLO	C_v	M_v	EWS	WD	DC
Weight	0.22	0.22	0.1	0.1	0.05	0.14	0.07	0.1

Table 5

Classification categories of offshore wind energy resource.

Class	Categorization value	Resource potential
1	$x \leq 0.4$	Poor
2	$0.4 \leq x \leq 0.5$	Marginal
3	$0.5 \leq x \leq 0.6$	Fair
4	$0.6 \leq x \leq 0.7$	Good
5	$0.7 \leq x \leq 0.8$	Excellent
6	$0.8 \leq x \leq 0.9$	Outstanding
7	$x > 0.9$	Superb

offshore WPD values were detected in the northwestern corner of the region, being clearly lower in the southern. The same WPD spatial pattern was obtained in previous studies in the western Iberia that used CORDEX simulations [8] and simulations carried out with WRF model [9,12]. However, annual mean PV_{res} shows a different pattern since the highest values are observed in the south ($\sim 200 \text{ Wm}^{-2}$) (Fig. 3b), whilst the lowest values are detected in the north. The annual PV_{res} are in good agreement with what was detected by López et al. [31], who observed values around 150 Wm^{-2} in the northeastern area analyzed in this study. It should be highlighted that offshore wind energy resource shows higher values than offshore solar power resource. For this reason, the present analysis is focused on the analysis of WPD but considering PV_{res} as a complement to improve the quality of the offshore renewable resource.

Both offshore wind and solar power resource show a heterogeneous spatial pattern (Fig. 3). The WPD and PV_{res} temporal variability were analyzed in terms of monthly means (Fig. 4) calculated for three grid points located at different latitudes (depicted in Fig. 1). As expected, PV_{res} (Fig. 4, red line) shows a similar pattern in the three locations, with a maximum in summer and lower values during winter. However, WPD (Fig. 4, blue line) presents a different monthly pattern depending on the location. At the southernmost location, the annual peak was observed in July (Fig. 4c, blue line), whilst in the northernmost grid point the highest WPD occurs during winter and the lowest in June (Fig. 4a, blue line). Combining both resources (Fig. 4, green line) it can be seen that the power resource becomes more stable throughout the year at north and middle locations compared to the WPD resource alone, since the difference between the maximum and minimum is reduced. Also noteworthy is the pattern in the middle grid point (Fig. 4b), where the combined resource is totally stable during the first 8 months of the year.

The seasonal behavior of WPD (Fig. 5) and WPD combined with PV_{res} (Fig. 6) allows a better understanding of their spatial and temporal variability in the western Iberia. The highest WPD values ($\sim 1200 \text{ Wm}^{-2}$) are detected during winter (Fig. 5a), especially in the northwestern corner of Iberia. In fact, this area showed the highest WPD in all seasons. Similar WPD values, although slightly lower, were observed in spring

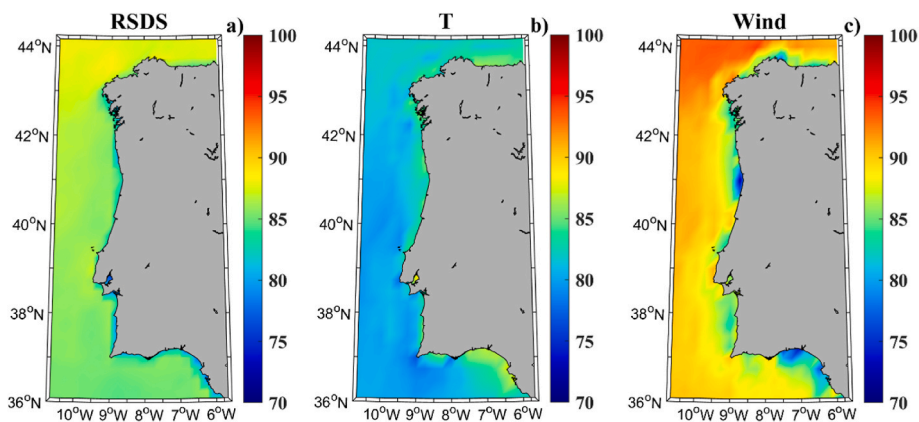


Fig. 2. Overlap percentage (OP, %) between ERA5 dataset and the multi-model ensemble of CORDEX simulations for the three variables used in the present analysis: (a) shortwave downward radiation, (b) temperature at 2 m, (c) wind speed at 10 m.

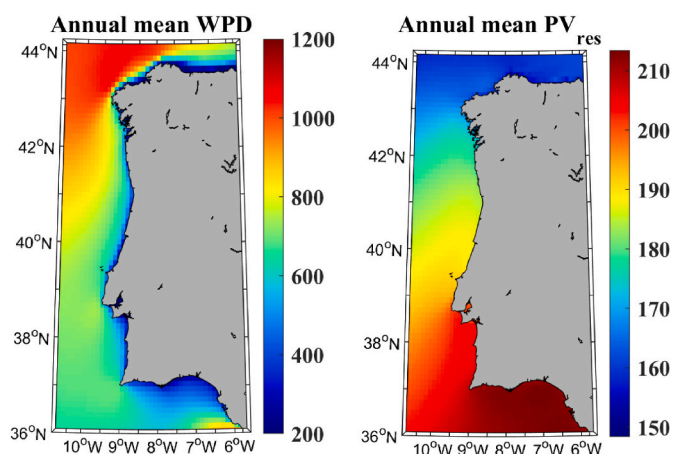


Fig. 3. (a) Annual mean WPD (Wm^{-2}) and (b) annual mean PV_{res} (Wm^{-2}) calculated using the multi-model CORDEX ensemble over the period 2000–2040.

(Fig. 5b). During summer (Fig. 5c), although the highest WPD values are found in the northwestern corner of Iberia, high WPD values around Cape Roca and Cape St. Vincent should be noted. Finally, autumn (Fig. 5d) is the season with the lowest WPD. Salvação and Soares [9] investigated offshore seasonal WPD over the period 2008–2013 for Iberia using a WRF model simulation and detected a similar pattern, for all seasons, to the one shown in Fig. 5. Costoya et al. [8] found a similar offshore WPD pattern, although the highest summer WPD values were found in the central and southern areas of western Iberia. These relatively small differences can be explained by the different set of simulations and time period under study (2085–2100 in Costoya et al. [8]).

The combination of WPD and PV_{res} results not only in higher power resource, as expected, but also a more spatially homogenous seasonal pattern (Fig. 6). This fact is especially visible in summer (Fig. 6c) when the entire western area of the Iberian Peninsula showed similar values around $\sim 1000 \text{ Wm}^{-2}$. In addition, the differences between the north and south areas are reduced during autumn (Fig. 6d). The reduction between maximum and minimum values observed in Fig. 4 in these two seasons is mainly related to the fact that the summer and autumn WPD values (Fig. 5) are the lowest throughout the year, while PV_{res} is the highest during these seasons (Fig. 4). This reduction in the amplitude of offshore energy potential when WPD and PV_{res} are considered together was also detected by López et al. [31] for the north of the Iberian Peninsula.

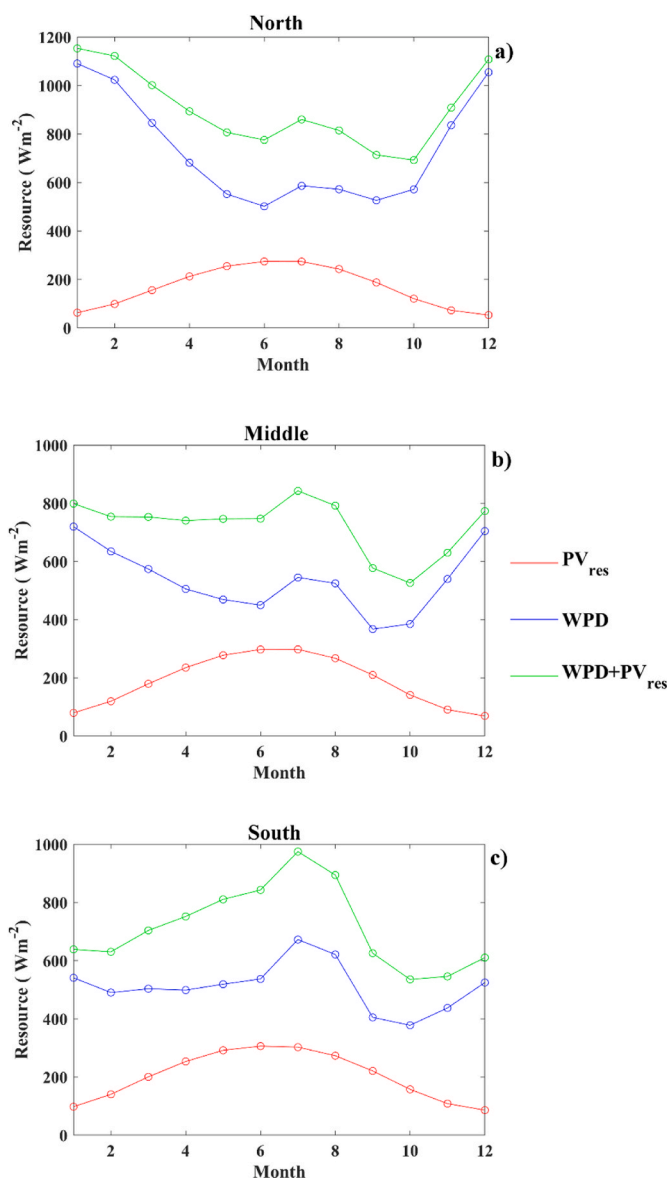


Fig. 4. Monthly series obtained by means of the CORDEX ensemble over the period 2000–2040 of WPD (blue line), PV_{res} (red line) and its sum (green line) for three different grid points (Fig. 1, white dots) located at the (a) north, (b) middle and (c) south of the area under scope.

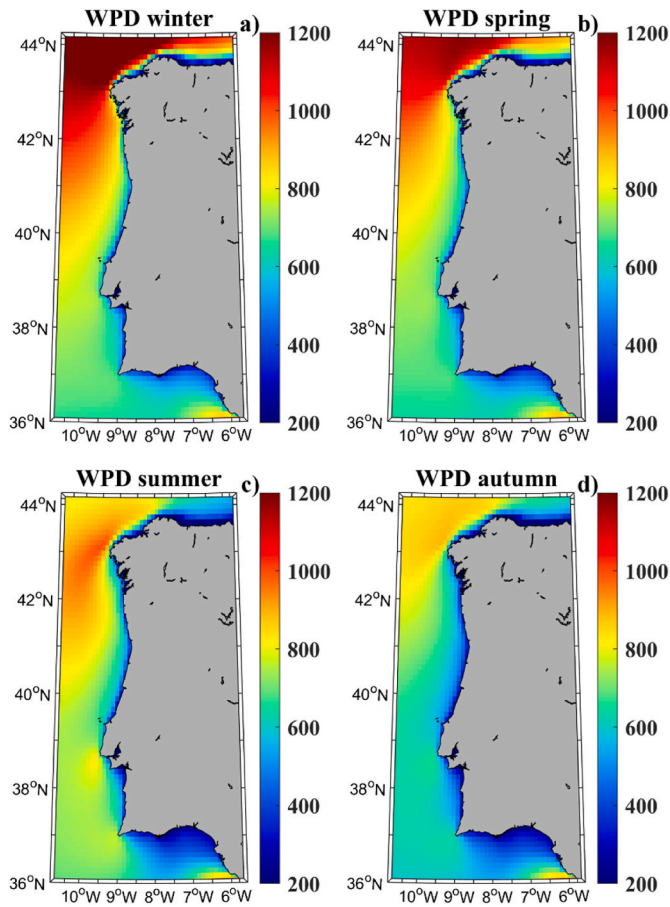


Fig. 5. Seasonal mean of the WPD multi-model ensemble (Wm^{-2}) for (a) winter (JDF), (b) spring (MAM), (c) summer (JJA) and (d) autumn (SON) over the period 2000–2040.

3.3. Offshore energy resource classification

Offshore energy classification was carried out considering stability, resource, risk, and economic factors. As a first step, classification was done by considering only WPD (Fig. 7). After the normalization process, values around 0.7 were obtained in most of the study area (Fig. 7a). Following Table 5, these values were translated into different classes. Most western Iberia was classified in Category 5, which is considered as excellent (Fig. 7b). However, it can be seen a fringe along the shoreline that was classified in Category 4 (good) or 3 (fair), especially in the northern and southern coastal areas. Similar values were observed by Ribeiro et al. [33], who classified offshore wind energy based on a multi-model ensemble with 7 RCMs from EURO-CORDEX project. These authors analyzed each of the eight indices separately and found the lowest values for the indices related to the depth (economic factor) and stability of the offshore wind energy resource. It is expected that the problems associated with the narrow continental shelf in western Iberia will be solved by implementing floating offshore wind farms, as discussed previously. However, a possible solution to improve the stability of the offshore renewable resource is to combine WPD with other renewable energy sources, particularly solar PV as shown in the present study.

The indices regarding the stability of the offshore wind energy resource (WPD only) throughout the year are shown in Fig. 8. In accordance with the analysis performed by Ribeiro et al. [33] low values were found for C_v index (Fig. 8a). This fact confirms that one of the main drawbacks of offshore wind energy exploitation in western Iberia is its inter-annual variability/seasonality, which is a relevant factor for an efficient supply of the produced energy to the grid. Low C_v values were

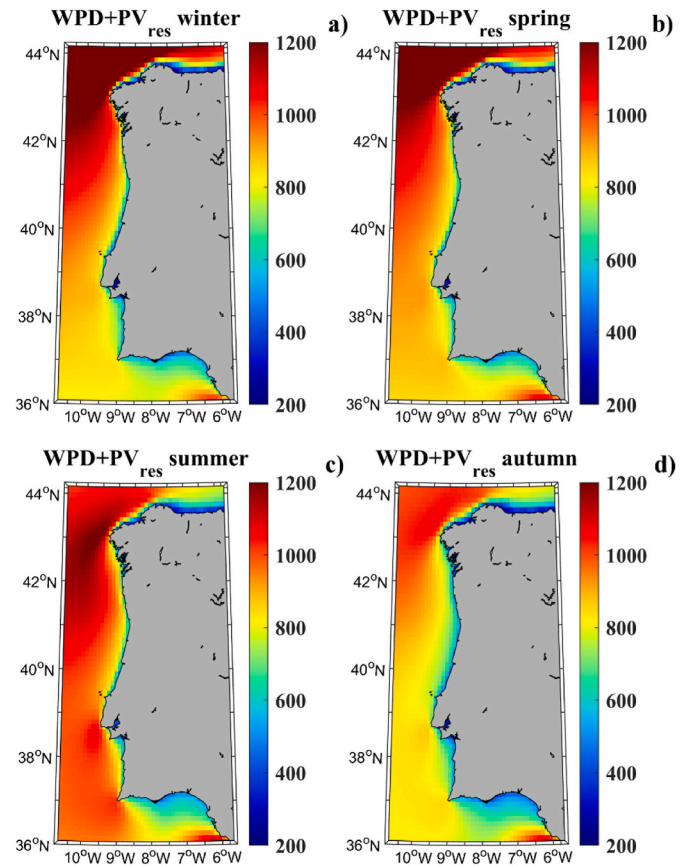


Fig. 6. Seasonal mean of $WPD + PV_{res}$ (Wm^{-2}) multi-model ensemble for (a) winter (JDF), (b) spring (MAM), (c) summer (JJA) and (d) autumn (SON) over the period 2000–2040.

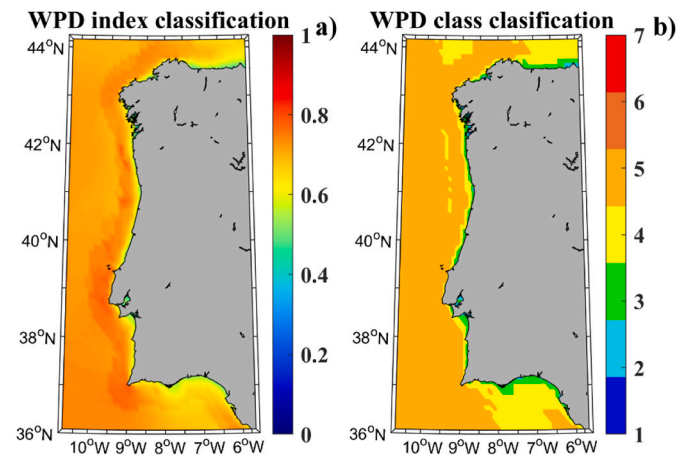


Fig. 7. Wind energy classification of the offshore wind energy resource by means of the multi-model ensemble of EURO-CORDEX simulations over the period 2000–2040. (a) WPD index classification and (b) WPD class classification.

partially compensated by M_v index that clearly showed higher values in the whole area (Fig. 8b). Stability indices recalculated considering together wind and solar offshore energy resources (Fig. 9) show substantially higher values. C_v index (Fig. 9a) increases from low values (0.35–0.55) (Fig. 8a) to medium or even high values (~0.8), especially in the coastal areas close to the shoreline and in the southernmost part. Regarding M_v index (Fig. 9b), higher values close one was found combining both resources.

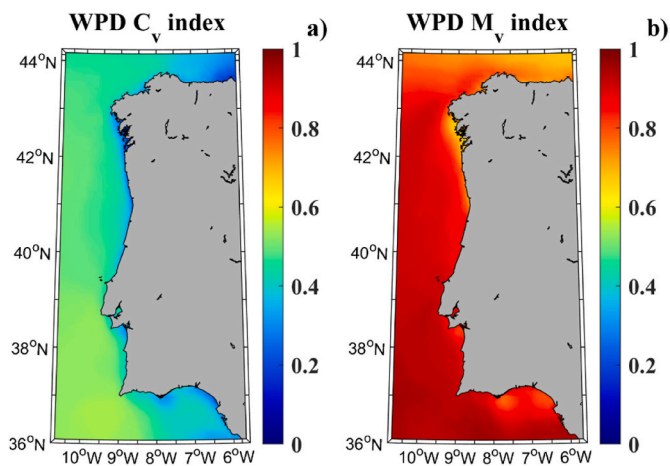


Fig. 8. Stability indices, (a) C_v and (b) M_v , calculated considering only WPD over the period 2000–2040.

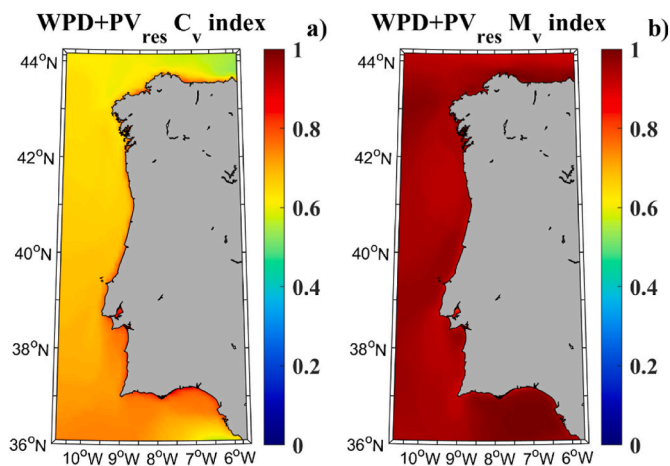


Fig. 9. Stability indices, (a) C_v and (b) M_v , calculated combining WPD and PV_{res} offshore resources over the period 2000–2040.

The impact of PV solar energy resource on the stability indices in the global class classification can be investigated considering the eight factors but taking into account C_v and M_v indices after combining WPD

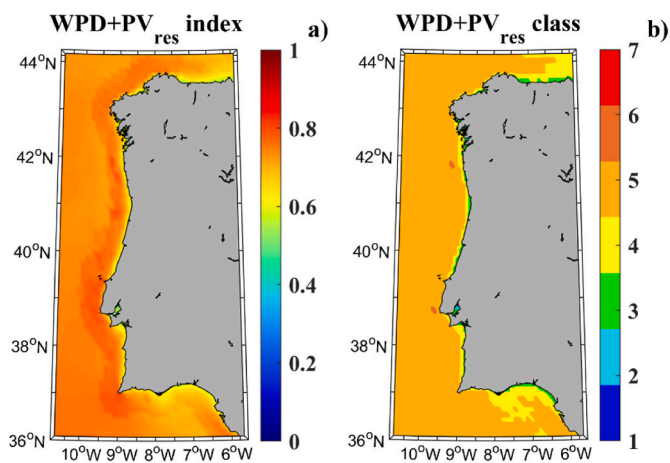


Fig. 10. Offshore energy resource classification combining WPD and PV_{res} by means of the multi-model ensemble of EURO-CORDEX simulations over the period 2000–2040. (a) WPD + PV_{res} index classification and (b) WPD + PV_{res} class classification.

and PV_{res} resources (Fig. 10). Fig. 10 is the same as Fig. 7 but considering the values of Fig. 9 for stability indices. In general, the main difference is that the Category 5 (excellent) area is higher (Fig. 10b). To better visualize the differences between the classification index and the class classification before and after considering WPD in combination with PV_{res} for the stability indices (C_v and M_v), they were subtracted in Fig. 11. Thus, Fig. 11a represents the difference between Figs. 10a and 7a, while Fig. 11b is the result of subtracting Figs. 7b to 10b. It can be seen that the combination of WPD and PV_{res} resources improves the classification in the entire area, but mainly along the coastal fringe with an increase of ~5%. This is a very important fact since the closest area to land is where future offshore wind farms are planned to be installed. An increase of one class is observed in some areas, mainly in the southern area of Portugal and also in the northern area of the Iberian Peninsula (Fig. 11b).

4. Discussion

Renewable energy technologies previously developed inland such as wind and solar photovoltaic can be adapted for offshore application, where there are larger areas for renewable energy farms with higher and more stable power density. Offshore wind farms on the western coast of the Iberian Peninsula are a promising alternative to increase the future supply of renewable energy by reducing the dependence on imported energy from outside Europe. Technical advances have led to the commercial exploitation of the first floating offshore wind farm in this area [7]. However, other drawbacks intrinsic to wind energy persist. One of them is its inter-annual variability, which may hinder the further development of this marine renewable energy in future planning processes. The present study has shown that the combination of offshore wind and solar photovoltaic energy clearly improves the stability of the energy resource throughout the year (Figs. 4 and 6). Thus, when the offshore wind energy resource was classified according to different factors (richness, economic cost, stability, and risk) an increase in the final classification index was observed (Fig. 11), especially in waters near the coast, caused by the improvement in stability indices (Fig. 9). This improvement offset the projected WPD decrease in western Iberia throughout the 21st century [8,13,14].

The analysis of the positive effects of combining offshore wind and solar PV energy was carried out over the period 2000–2040 because this approach considers the impact of climate change over both renewable resources but also because it is expected that offshore wind farms and especially offshore PV solar panels will reach the necessary degree of maturity in the upcoming decades. This is a relevant fact because it is difficult to predict how this technology will evolve in the next years to

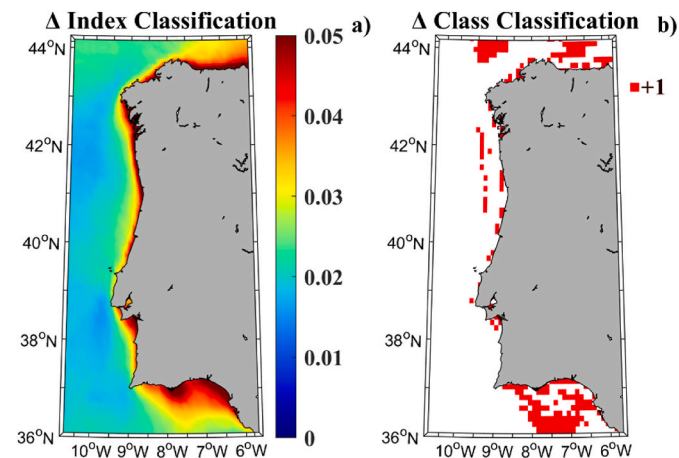


Fig. 11. Changes in offshore renewable energy classification: (a) total index and (b) class increase after considering stability indices (C_v and M_v) from combining WPD + PV_{res} .

deal with the marine environment, which could involve, for example, higher maintenance costs or some type of protection for the PV solar panels. This fact can suppose that offshore PV solar presents higher values of Levelized Cost of Energy than onshore PV solar, although the efficiency of the first one is higher ([25]). Apart from economic uncertainties, it is important to have in mind that other restrictions derived from the protection of different interests such as biodiversity protection, fishing, or navigation [16,58] condition the possible areas where an offshore hybrid farm can be deployed. Due to these economic and legal uncertainties, whose analysis are out of the scope of the present study, this manuscript is focused on the available wind and solar resource and the classification index only considers economic factors that will remain inalterable in the upcoming decades, such as water depth or distance to the coast. In addition, it is important to note that both wind turbines and PV panels will likely become more efficient in the upcoming decades, and it is not feasible to realistically anticipate these future improvements. For these reasons, the present study is focused on the resource (WPD and PV_{res}) and not on the expected power output. Power resource was calculated in terms of WPD for wind energy and PV_{res} for PV solar energy, both in the same units (Wm^{-2}). Both metrics are independent of the available technology since WPD and PV_{res} represent the maximum amount of energy that can be drawn from each renewable source per area unit, and do not depend on a specific wind turbine or a PV panel technology or model. However, the calculation of WPD was carried out assuming an offshore floating turbine with 120 m of approximate hub height, which is commercially available in 2021 [41]. A different assumption of turbine hub height would result in different wind resource assessment values per square meter. Also, the PV_{res} were calculated assuming a PV power performance ratio varying linearly on a typical constant of $-0.005\text{ }^{\circ}C^{-1}$, based on monocrystalline silicon solar panels [45]. These assumed values are typical, i.e., not from a specific wind turbine or PV model. Using WPD and PV_{res} metrics fits the purpose of this study, which is to analyze the advantages of combining both renewable resources in terms of the resource richness and stability, which is intrinsic to each location and not directly dependent on the technology used to generate power (although the effective generated power is obviously dependent on the type of technology used).

Therefore, it is important to mention that the present manuscript represents the first step in the development of offshore hybrid systems based on wind and PV solar resource on the western Iberian Peninsula. The current study showed that the combination of offshore wind and PV solar energy improved the stability of the resource along the year. This fact is especially relevant since the Iberian Peninsula remains largely an energy island due to a low level of interconnection with the European electricity market [59]. It should not be forgotten that the final aim of improving the stability of the energy supply is to maintain the supply-demand balance. At this point, it is interesting to mention that the combination of wind and solar energy can help maintain this balance, since the highest WPD was found during winter, while the highest PV_{res} occurred during summer (Fig. 4), coinciding with the months of the two annual peaks of the energy demand in the Spanish mainland (Fig. A.1, appendix). However, the latter phases of development of this hybrid system must be done at lower spatial scales considering, for example, legal restrictions derived from other sea uses. Moreover, an analysis of the variability of both renewable resources at a lower temporal resolution (hourly or daily) may be also addressed in future research since it is an important factor when planning a power generation system based on weather-dependent marine renewable energies. In this way, future analysis based on energy output can adapt the amount of wind turbines or PV solar panels to fit on the best way the supply-demand balance at daily and even hourly scales. Other parameters such as the hub height, which was assumed to be 120 m in the present analysis, also can help to modulate the wind energy output to cover the peaks demand since higher wind turbines are already being installed [41].

5. Concluding remarks

This study investigated the advantages of a hybrid wind-PV solar offshore energy system in the western Iberian Peninsula in the context of climate change over the period 2000–2040. The classification of the combined energy resource was carried out using a Delphi method applied to eight indices that relate to four categories: stability of the resource, richness of the offshore resource, economic factors, and risk factors. These indices were calculated using a multi-model ensemble composed by 35 simulations from the EURO-CORDEX project. To our knowledge, the analysis here presented involves the highest number of simulations in an offshore energy resource analysis performed using EURO-CORDEX data.

The main findings of this study can be summarized as follows:

- The reliability of each EURO-CORDEX simulation to represent wind speed, air temperature and shortwave downward radiation was proved by comparing with data from ERA5 dataset.
- Offshore wind energy resource is greater than the PV solar one in the western Iberian Peninsula. Both renewable sources showed high spatial and temporal variability throughout the year.
- The combination of solar photovoltaic and wind energy resources in a hybrid offshore wind-PV solar farm, significantly improves the total renewable energy resource and reduces the spatial and temporal variability of both individual energy resources, which is of crucial importance for a more efficient and optimized use of energy derived from renewable sources.
- During summer, the entire area has an offshore wind-PV solar resource greater than 800 kW m^{-2} . During winter, the northern region has a greater resource than the south, with values between 900 and 1000 kW m^{-2} .
- Offshore wind energy resource is rated as excellent in most of the region, except in the coastal areas closest to shore where it is rated as good or fair. When the stability of the resource is improved by combining PV solar and wind energy, the total index classification increases, especially along the coastal fringe closest to land where it the lowest rating is of “good”.
- Some areas located north and south of the Iberian Peninsula improved their final classification by one level after considering the hybrid offshore wind-PV solar energy production system concept.

Technical advances in offshore marine energy have already allowed the installation of floating offshore wind farms, and other advances are currently under testing such as the use of floating PV solar farms. In this sense, rapid growth in the installation of offshore wind farms is expected in the west of the Iberian Peninsula in the next decades.

The present analysis showed significant advantages in combining these two renewable sources, with PV solar energy showing an interesting ability to solve one of the main drawbacks of wind energy - its lack of stability to supply the energy network throughout the year due to its high inter-annual (seasonal) variability. These aspects are paramount in the decision making and planning processes of renewable energy production systems that will be developed in the upcoming decades in western Iberia. This analysis is a first step in the development of offshore wind and PV solar systems. Future research should analyze the legal constraints for the installation of offshore platforms and the balance between supply and demand should be studied at a lower temporal resolution (hourly or daily) in later phases of the planning process.

Credit author statement

Xurxo Costoya: Conceptualization, Methodology, Software, Writing - Original Draft, Writing - Review & Editing, Data curation, Formal Analysis. **Maite deCastro:** Data curation, Software, Methodology, Resources, Formal Analysis. **David Carvalho:** Writing - Review & Editing, Investigation, Formal Analysis, Data curation. **Beatriz Arguilé-Pérez:**

Data curation, Visualization, Writing – review & editing. **Moncho Gómez-Gesteira**: Software, Supervision, Visualization.

Declaration of competing interest

The authors declare that they have no known competing financial interests or personal relationships that could have appeared to influence the work reported in this paper.

Acknowledgments

X. Costoya is supported by the Spanish Government through a Juan de la Cierva Postdoctoral Fellowship (FJCI-2017-32577). This work was partially supported by Xunta de Galicia under project ED431C 2021/44 (Grupos de Referencia Competitiva) and Ministry of Science and Innovation of the Government of Spain under the project SURVIWEC PID2020-113245RB-I00. D. Carvalho acknowledges the Portuguese Foundation for Science and Technology (FCT) for his researcher contract

(CEECIND/01726/2017) and the FCT/MCTES for the financial support to CESAM (UIDP/50017/2020+UIDB/50017/2020), through national funds.

The authors acknowledge the World Climate Research Programme's Working Group on Regional Climate, the Working Group on Coupled Modelling, the modelling groups listed in Table 1 of this paper for producing and making available their model output, the Earth System Grid Federation infrastructure (an international effort led by the U.S. Department of Energy's Program for Climate Model Diagnosis and Intercomparison), the European Network for Earth System Modelling and other partners in the Global Organisation for Earth System Science Portals (GO-ESSP). We also acknowledge ECMWF and the Copernicus Climate Change Service for providing and making available the ERA5 reanalysis data used in this work. Thanks are also due to the National Marine Science Data Centre of China (<http://mds.nmdis.org.cn/>), the National Science and Technology Resource Sharing Service Platform, for providing data support.

APPENDIX

Table A.1

Overlap percentage (OP, in %) between CORDEX simulations and ERA5 dataset for PV_{res} (second column) and WPD (third column). Last row represents the multi-model mean of the OP and its standard deviation.

Model Number	PV_{res} OP	WPD OP
1	89.93	91.81
2	86.37	86.19
3	87.16	88.01
4	83.16	89.24
5	79.42	86.09
6	87.86	87.75
7	91.58	87.38
8	87.95	89.48
9	86.25	89.01
10	91.61	88.53
11	80.75	92.31
12	80.69	83.11
13	85.20	91.10
14	90.31	90.26
15	89.01	90.44
16	81.87	89.60
17	87.08	89.59
18	86.34	88.49
19	79.90	88.57
20	88.04	93.06
21	90.49	93.28
22	87.64	90.10
23	79.72	89.40
24	83.55	87.32
25	85.15	88.38
26	87.26	82.86
27	85.50	88.35
28	80.36	90.21
29	91.85	87.46
30	81.82	92.35
31	86.94	91.36
32	84.86	93.28
33	79.43	90.75
34	87.41	91.11
35	92.38	91.99
Total mean	85.85 ± 3.92	89.38 ± 2.50

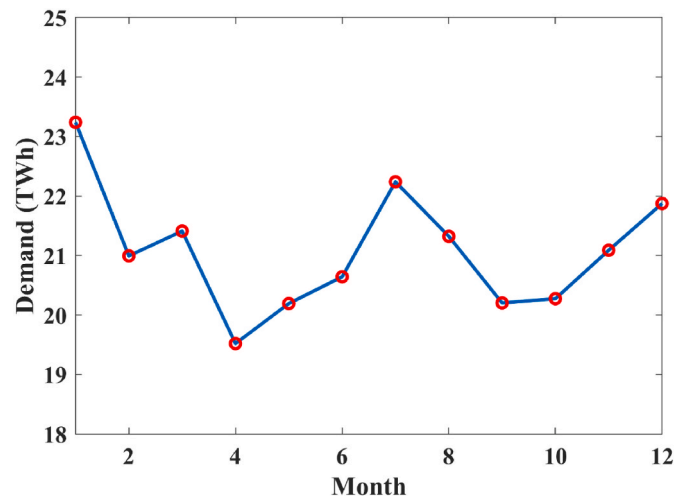


Fig. A.1. Monthly energy demand in mainland Spain (TWh) averaged over the period 2011–2020. Data was provided by the Spanish Electricity System (<https://www.ree.es/en>).

References

- [1] European Commission. Communication from the commission to the European parliament, the Council, the European economic and social committee and the committee of the regions. A policy framework for climate and energy in the period from 2020 to 2030. 2014. Available at: <https://eur-lex.europa.eu/legal-content/EN/ALL/?uri=CELEX:52014DC0015>. [Accessed 18 May 2021].
- [2] European Commission. Regulation of the European parliament and of the council establishing the framework for achieving climate neutrality and amending regulation (EU) 2018/1999 (European climate law). 2020. Available at: <https://eur-lex.europa.eu/legal-content/EN/TXT/?uri=CELEX:52020PC0080>. [Accessed 18 May 2021].
- [3] IRENA, International Renewable Energy Agency. Renewable capacity statistics 2020. 2020. Available online: <https://irena.org/publications/2020/Mar/Renewable-Capacity-Statistics-2020>. [Accessed 14 April 2021].
- [4] Ramos V, Giannini G, Calheiros-Cabral T, Rosa-Santos P, Taveira-Pinto F. Legal framework of marine renewable energy: a review for the Atlantic region of Europe. *Renew Sustain Energy Rev* 2021;137:110608.
- [5] ETIPOCEAN. Strategic research and innovation agenda for ocean energy. 2020. Brussels, Belgium. Available at: <https://www.oceanenergy-europe.eu/wp-content/uploads/2020/05/ETIP-Ocean-SRIA.pdf>. [Accessed 14 April 2021].
- [6] GWEC. Global offshore wind report 2020. Global Wind Energy Council; 2020. Available at: <https://gvec.net/global-offshore-wind-report-2020/>. [Accessed 15 April 2021].
- [7] Ramírez L, Fraile D, Brindley G. Offshore wind in Europe: key trends and statistics 2020. 2021. Available at: <https://windeurope.org/intelligence-platform/product/offshore-wind-in-europe-key-trends-and-statistics-2020/>. [Accessed 15 April 2021].
- [8] Costoya X, Rocha A, Carvalho D. Using bias-correction to improve future projections of offshore wind energy resource: a case study on the Iberian Peninsula. *Appl Energy* 2020;262:114562.
- [9] Salvação N, Soares CG. Wind resource assessment offshore the Atlantic Iberian coast with the WRF model. *Energy* 2018;145:276–87.
- [10] Carvalho D, Rocha A, Gómez-Gesteira M, Alvarez I, Santos CS. Comparison between CCMP, QuikSCAT and buoy winds along the Iberian Peninsula coast. *Remote Sens Environ* 2013;137:173–83.
- [11] Carvalho D, Rocha A, Gómez-Gesteira M, Santos CS. Comparison of reanalyzed, analyzed, satellite-retrieved and NWP modelled winds with buoy data along the Iberian Peninsula coast. *Remote Sens Environ* 2014;152:480–92.
- [12] Carvalho D, Rocha A, Gómez-Gesteira M, Santos CS. Offshore winds and wind energy production estimates derived from ASCAT, OSCAT, numerical weather prediction models and buoys—A comparative study for the Iberian Peninsula Atlantic coast. *Renew Energy* 2017;102:433–44.
- [13] Soares PM, Lima DC, Cardoso RM, Nascimento ML, Semedo A. Western Iberian offshore wind resources: more or less in a global warming climate? *Appl Energy* 2017;203:72–90.
- [14] Santos F, Gómez-Gesteira M, deCastro M, Añel JA, Carvalho D, Costoya X, Dias JM. On the accuracy of CORDEX RCMs to project future winds over the Iberian Peninsula and surrounding ocean. *Appl Energy* 2018;228:289–300.
- [15] Rodríguez-Rodríguez D, Malak DA, Soukissian T, Sánchez-Espinosa A. Achieving Blue Growth through maritime spatial planning: offshore wind energy optimization and biodiversity conservation in Spain. *Mar Pol* 2016;73:8–14.
- [16] Salvador S, Costoya X, Sanz-Larruga FJ, Gimeno L. Development of offshore wind power: contrasting optimal wind sites with legal restrictions in Galicia, Spain. *Energies* 2018;11(4):731.
- [17] Castro-Santos L, Filgueira-Vizoso A, Carral-Couce L, Formoso JÁF. Economic feasibility of floating offshore wind farms. *Energy* 2016;112:868–82.
- [18] Castro-Santos L, deCastro M, Costoya X, Filgueira-Vizoso A, Lamas-Galdo I, Ribeiro A, Gómez-Gesteira M. Economic feasibility of floating offshore wind farms considering near future wind resources: case study of Iberian Coast and Bay of Biscay. *Int J Environ Res Publ Health* 2021;18(5):2553.
- [19] Katsaprakakis DA, Christakis DG. Seawater pumped storage systems and offshore wind parks in islands with low onshore wind potential. A fundamental case study. *Energy* 2014;66:470–86.
- [20] Astariz S, Vazquez A, Iglesias G. Evaluation and comparison of the levelized cost of tidal, wave, and offshore wind energy. *J Renew Sustain Energy* 2015;7(5):053112.
- [21] Roy A, Auger F, Dupriez-Robin F, Bourguet S, Tran QT. Electrical power supply of remote maritime areas: a review of hybrid systems based on marine renewable energies. *Energies* 2018;11(7):1904.
- [22] Golroodbari SZM, Vaartjes DF, Meit JBL, van Hoeken AP, Eberveld M, Jonker H, van Sark WJHM. Pooling the cable: a techno-economic feasibility study of integrating offshore floating photovoltaic solar technology within an offshore wind park. *Sol Energy* 2021;219:65–74.
- [23] Tiong YK, Zahari MA, Wong SF, Dol SS. The feasibility of wind and solar energy application for oil and gas offshore platform. *IOP Conf Ser Mater Sci Eng* 2015;78. <https://iopscience.iop.org/article/10.1088/1757-899X/78/1/012042>.
- [24] Wu Y, Li L, Song Z, Lin X. Risk assessment on offshore photovoltaic power generation projects in China based on a fuzzy analysis framework. *J Clean Prod* 2019;215:46–62.
- [25] Golroodbari SZ, van Sark W. Simulation of performance differences between offshore and land-based photovoltaic systems. *Progr Photovolt* 2020;28(9):873–86.
- [26] Oliveira-Pinto S, Rosa-Santos P, Taveira-Pinto F. Assessment of the potential of combining wave and solar energy resources to power supply worldwide offshore oil and gas platforms. *Energy Convers Manag* 2020;223:113299.
- [27] Trapani K, Millar DL. Proposing offshore photovoltaic (PV) technology to the energy mix of the Maltese islands. *Energy Convers Manag* 2013;67:18–26. 2013.
- [28] Gorjian S, Sharon H, Ebadi H, Kant K, Scavo FB, Tina GM. Recent technical advancements, economics and environmental impacts of floating photovoltaic solar energy conversion systems. *J Clean Prod* 2020;124:285.
- [29] Oceans of Energy. A world's first: offshore floating solar farm installed at the Dutch North Sea - oceans of Energy. 2019. Available at: <https://oceansofenergy.blue/2019/12/11/a-worlds-first-offshore-floating-solar-farm-installed-at-the-dutch-north-sea/>. [Accessed 16 April 2021].
- [30] Folkers W, van Sark W, de Keizer C, van Hoof W, van den Donker M, Roadmap pv systems and applications. Study commissioned by The Netherlands enterprise agency (RVO) in collaboration with the TKI urban. Energy; 2017.
- [31] López M, Rodríguez N, Iglesias G. Combined floating offshore wind and solar PV. *J Mar Sci Eng* 2020;8(8):576.
- [32] Solanki C, Nagababu G, Kachhwaha SS. Assessment of offshore solar energy along the coast of India. *Energy Proc* 2017;138:530–5.
- [33] Ribeiro A, Costoya X, de Castro M, Carvalho D, Dias JM, Rocha A, Gomez-Gesteira M. Assessment of hybrid wind-wave energy resource for the NW coast of Iberian Peninsula in a climate change context. *Appl Sci* 2020;10(21):7395.
- [34] Jacob D, Teichmann C, Sobolowski S, Katragkou E, Anders I, Belda M, Wulfmeyer V. Regional climate downscaling over Europe: perspectives from the EURO-CORDEX community. *Reg Environ Change* 2020;20(2):1–20.
- [35] Hennemuth TI, Jacob D, Keup-Thiel E, et al. Guidance for EURO-CORDEX climate projections data use. 2017. Available at: <https://www.euro-cordex.net/imperia/md/content/csc/cordex/euro-cordex-guidelines-version1.0-2017.08.pdf>. [Accessed 8 April 2021].

- [36] Hersbach H, Bell B, Berrisford P, Hirahara S, Horányi A, Muñoz-Sabater J, Simmons A. The ERA5 global reanalysis. *Q J R Meteorol Soc* 2020;146(730):1999–2049.
- [37] Ramon J, Lledó L, Torralba V, Soret A, Doblas-Reyes FJ. What global reanalysis best represents near-surface winds? *Q J R Meteorol Soc* 2018;145(724):3236–51.
- [38] Costoya X, deCastro M, Carvalho D, Feng Z, Gómez-Gesteira M. Climate change impacts on the future offshore wind energy resource in China. *Renew Energy* 2021;175:731–47.
- [39] Perkins SE, Pitman AJ, Holbrook NJ, McAneney J. Evaluation of the AR4 climate models' simulated daily maximum temperature, minimum temperature, and precipitation over Australia using probability density functions. *J Clim* 2007;20(17):4356–76.
- [40] Costoya X, deCastro M, Santos F, Sousa MC, Gómez-Gesteira M. Projections of wind energy resources in the Caribbean for the 21st century. *Energy* 2019;178:356–67.
- [41] Musial W, Beiter P, Schwabe P, Tian T, Stehly T, Spitsen P. 2016 offshore wind technologies market report. Washington, D.C.: U.S. Department of Energy, Office of Energy Efficiency & Renewable Energy; 2017. DOE/GO-102017-5031, <https://www.energy.gov/eere/wind/downloads/2016-offshore-wind-technologies-market-report>.
- [42] Leon JM, Koivisto MJ, Sørensen P, Magnant P. Power fluctuations in high installation density offshore wind fleets. *Wind Energy Science Discussions*; 2020. p. 1–23. 2020.
- [43] Radziemska E. The effect of temperature on the power drop in crystalline silicon solar cells. *Renew Energy* 2003;28(1):1–12.
- [44] Jerez S, Tobin I, Vautard R, Montávez JP, López-Romero JM, Thais F, Wild M. The impact of climate change on photovoltaic power generation in Europe. *Nat Commun* 2015;6(1):1–8.
- [45] Tonui JK, Tripanagnostopoulos Y. Performance improvement of PV/T solar collectors with natural air flow operation. *Sol Energy* 2008;82(1):1–12.
- [46] Chenni R, Makhoul M, Kerbache T, Bouzid A. A detailed modeling method for photovoltaic cells. *Energy* 2007;32(9):1724–30.
- [47] Pierce DW, Barnett TP, Santer BD, Gleckler PJ. Selecting global climate models for regional climate change studies. *Proc Natl Acad Sci Unit States Am* 2009;106(21):8441–6.
- [48] Jacob D, Petersen J, Eggert B, Alias A, Christensen OB, Bouwer LM, Yiou P. EURO-CORDEX: new high-resolution climate change projections for European impact research. *Reg Environ Change* 2014;14(2):563–78.
- [49] Zheng CW, Xiao ZN, Peng YH, Li CY, Du ZB. Rezoning global offshore wind energy resources. *Renew Energy* 2018;129:1–11.
- [50] Costoya X, deCastro M, Carvalho D, Gómez-Gesteira M. On the suitability of offshore wind energy resource in the United States of America for the 21st century. *Appl Energy* 2020;262:114537.
- [51] National Renewable Energy Laboratory (NREL). Wind Energy resource atlas of the United States. DOE/CH. October 1986. p. 10093–4. <http://redc.nrel.gov/wind/pubs/atlas>. [Accessed 13 April 2021].
- [52] Zheng CW, Pan J, Li JX. Assessing the China Sea wind energy and wave energy resources from 1988 to 2009. *Ocean Eng* 2013;65:39–48.
- [53] Zheng CW, Pan J. Assessment of the global ocean wind energy resource. *Renew Sustain Energy Rev* 2014;33:382–91.
- [54] Wessel P, Smith WH. A global, self-consistent, hierarchical, high-resolution shoreline database. *J Geophys Res Solid Earth* 1996;101(B4):8741–3.
- [55] NOAA National Geophysical Data Center. ETOPO1 1 arc-minute global relief model. NOAA National Centers for Environmental Information; 2009. . [Accessed 13 April 2021].
- [56] Coles S. An introduction to statistical modeling of extremes. London: Springer-Verlag; 2001.
- [57] Castillo E, Hadi AS, Balakrishnan N, Sarabia JM. Extreme value and related models with applications in engineering and science. New Jersey: John Wiley & Sons; 2004.
- [58] deCastro M, Costoya X, Salvador S, Carvalho D, Gómez-Gesteira M, Sanz-Larruga FJ, Gimeno L. An overview of offshore wind energy resources in Europe under present and future climate. *Ann N Y Acad Sci* 2019;1436(1):70–97.
- [59] European Commission. Integration of the Iberian Peninsula into the internal energy market. Brussels: European Commission Fact Sheet; 2018. Available at: https://ec.europa.eu/commission/presscorner/detail/en/MEMO_18_4622.